Ukrainian Journal of Physical Optics
ISSUE 1
2024

A NEW FILTERLESS W-BAND MILLIMETER WAVE SIGNALS GENERATION SCHEME WITH FREQUENCY OCTUPLING BASED ON CASCADED MACH–ZEHNDER MODULATORS

DONGFEI WANG[1,2,3,*], YU ZHANG[4,5], ZUFANG YANG[1], LAN ZHANG[1], BAOHONG WU[1], XIAOKUN YANG[2], SHUXIA YAN[6], XIANGQING WANG[1,7]

[1] School of Artificial Intelligence, Wuhan Technology and Business University, Wuhan, 430065, China, wdfchina@126.com
[2] School of Electronics and Information, Nanchang Institute of Technology, Nanchang, Jiangxi Province, 330044, China
[3] School of Information Engineering, Beijing Institute of Graphic Communication, Beijing 102600 China
[4] Jincheng Research Institute of Opto-mechatronics Industry, Jincheng 048000, China
[5] Shanxi Key Laboratory of Advanced Semiconductor Optoelectronic Devices and Integrated Systems, Jincheng 048000, China
[6] Tianjin Key Laboratory of Optoelectronic Detection Technology and System, Tianjin 300387 China
[7] Henan Key Laboratory of Visible Light Communications, Zhengzhou, China
* wdfchina@126.com

Received: 24.12.2023

Abstract. The existing frequency bands, such as the C-band and L-band, are becoming increasingly crowded and cannot meet the growing demand for high-speed data rate services. To overcome spectrum congestion, meet future business needs, and overcome the bottlenecks of traditional electronic methods, we have modified an approach for generating W-band mm-wave signals with octupling frequency without the need for an optical filter. One integrated modulator consisting of two push-pull Mach–Zehnder modulators (MZM) in series is employed to achieve W-band signal generation. The octupling frequency signal generation depends on ±4th optical sidebands to beat frequency in the photodetector. For capturing ±4th optical sidebands, the bias point of the two push-pull MZMs needs work at the peak point, and the modulation index of the two MZMs should be simultaneously set to 2.4. We have conducted detailed mathematical derivation and computer simulation for the scheme, demonstrating its correctness. The results show that the optical sideband suppression ratio is not less than 45.73 dB, and the RF sideband suppression ratio can reach 37.64 dB.

Keywords: W-band, mm-wave signal generation, frequency octupling, Mach–Zehnder modulator
UDC: 535.8
DOI: 10.3116/16091833/Ukr.J.Phys.Opt.2024.01085

1. Introduction

Millimeter-wave (mm-wave) range is a band for emerging wireless communication technology, with a frequency range between 30 and 300 GHz [1-3]. Compared to traditional wireless communication technology, millimeter wave technology has higher bandwidth and faster transmission speed, which can achieve more efficient data transmission and lower latency [4-7]. Millimeter wave technology can also achieve higher spectral efficiency, enabling more data transmission within limited spectral resources, which can be used for communication [8-9], in short-range radars [10-11], in sensors [12-13], in scanners of airport security [14-15], etc. Due to the electronic "bottleneck problem," traditional electronic methods and technologies have many limitations in generating mm-wave signals,

such as large volume, high-frequency loss, small instantaneous bandwidth, and severe electromagnetic interference [16-20]. Compared to others, mm-wave signals generation based on photonic technique can cover relatively wideband, and it is inherently compatible with radio-over-fiber (ROF) systems, which achieve high-capacity and low-cost wired transmission of RF signals, and ultra-wideband wireless data transmission. Hence, photonic or optical schemes to generate mm-wave signals have drawn much attention recently.

A large number of research achievements have emerged in the current generation of mm-wave signals based on photon technologies, to which belong optical heterodyne technology [21-22], direct modulation technology based on direct modulators, frequency-up conversion technology based on nonlinear effects, such as stimulated Brillouin scattering [23] and four-wave mixing [24-25], and external modulation technology based on electro-absorption modulators, phase modulators [26-27], Mach–Zehnder modulators (MZM) [28-31], dual parallel MZM [32-35] or cascaded MZM [36-38]. Among these approaches, external modulation techniques have been widely exploited and studied. Using external modulators cascaded with a filter or wavelength select switch, frequency doubling [39], quadrupling [40], and even octupling mm-wave could be obtained. A higher order harmonic frequency is needed to get a higher frequency mm-wave, while the scheme of mm-wave generation will be more complicated and of low quality. Some works on octupling frequency mm-wave generation have been reported. In [41], authors employed cascading a Sagnac loop with an intensity modulator and a dual-parallel MZM in series to generate octupling frequency mm-wave, and the optical sideband suppression ratio (OSSR) only ran to 20dB, and RF sideband suppression ratio (RFSSR) only attained 17 dB. In Ref.[42], mm-wave signals with frequency octupling have been proposed using two cascaded MZMs. This requires precise modulation index (MI) control to 2.4048, which is difficult to achieve in actual experiments. In Ref. [42], the key indicators OSSR and RFSSR have not been analyzed. In addition, it can be found from the spectral and radio frequency spectra presented in [42] that the quality of the signals is poor, with many signals of harmonic interference.

To overcome spectrum congestion, meet future business needs, and overcome the bottlenecks of traditional electronic methods, a frequency octupling scheme is proposed using only one integrated modulator consisting of two push-pull MZM cascades without an optical filter. Two fourth-order harmonics are generated in the output optical signal by appropriately adjusting the two MZMs bias voltages, the radio frequency driving voltages, and phases. The scheme was simulated and verified through computer software, which can result in using 10 GHz microwave driving signals to obtain W-band 80 GHz millimeter waves.

2. The theory principles of mm-wave signal generation

Fig. 1 reveals the schematic architecture of the proposed scheme for realizing W band signal generation by frequency octupling with no need for an optical filter. The continuous lightwave output from a laser is defined as $E_{\text{in}} = E_c \cos(\omega_c t)$, where E_{c} represents the amplitude of continuous lightwave, and ω_{c} is the angular frequency of continuous lightwave. An additional unmodulated light wave is added structurally to eliminate the influence of residual 0th-order optical harmonics, resulting in better and purer target W-band mm-wave signal generation quality. The electric phase shifter is set to 90 degrees to create a $\pi/2$ phase difference between the RF driving signals injected into two MZMs.

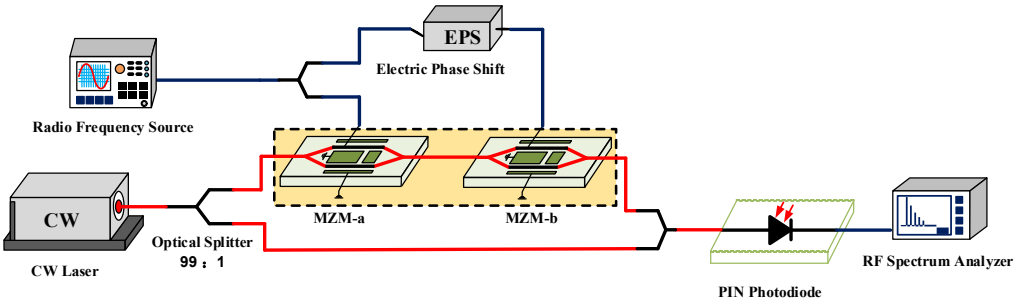

Fig. 1. Schematic architecture of W-band mm-wave generation with frequency octupling.

The light wave output by MZM-a can be given as

$$E_{MZM-a}=\frac{\gamma E_c}{2}\begin{bmatrix}-J_{-2}(\beta)e^{j(\omega_c-2\omega_m)t}-J_2(\beta)e^{j(\omega_c+2\omega_m)t}+J_{-4}(\beta)e^{j(\omega_c-4\omega_m)t}\\+J_4(\beta)e^{j(\omega_c+4\omega_m)t}-J_{-6}(\beta)e^{j(\omega_c-6\omega_m)t}-J_6(\beta)e^{j(\omega_c+6\omega_m)t}\cdots\end{bmatrix}. \quad (1)$$

Where $J_n(\beta)$ is the first kind n-th order Bessel function, β denotes the MI of the MZM defined as $\pi V_m/V_\pi$, V_m represents the amplitude of the RF driving signal, ω_m is the angular frequency of the RF driving signal, and V_π is the switching voltage of MZM. From Eq. (1), the 0th-order optical carrier and the odd-order optical harmonics are all eliminated, and only even-order optical harmonics are kept, except the 0th-order optical carrier. In addition to the strangulation of odd-order light sidebands, the 0th-order light sideband is also eliminated due to the MI being set to 2.4. The output by MZM-a is emitted into MZM-b, and the parameter of the optical phase shifter is configured to π. So that the 2nd and 6th-order optical harmonics of (4n-2)th order are suppressed. The output optical signal after MZM-b can be described as

$$\begin{aligned}E_{MZM-b}&=\frac{\gamma E_{MZM-a}}{2}\begin{bmatrix}J_{-2}(\beta)e^{j(-2\omega_m)t}+J_2(\beta)e^{j(+2\omega_m)t}+J_{-4}(\beta)e^{j(-4\omega_m)t}\\+J_4(\beta)e^{j(+4\omega_m)t}+J_{-6}(\beta)e^{j(-6\omega_m)t}+J_6(\beta)e^{j(+6\omega_m)t}\cdots\end{bmatrix}\\&=\frac{\gamma^2E_c}{4}\begin{bmatrix}-J_{-2}(\beta)e^{j(\omega_c-2\omega_m)t}-J_2(\beta)e^{j(\omega_c+2\omega_m)t}+J_{-4}(\beta)e^{j(\omega_c-4\omega_m)t}\\+J_4(\beta)e^{j(\omega_c+4\omega_m)t}-J_{-6}(\beta)e^{j(\omega_c-6\omega_m)t}-J_6(\beta)e^{j(\omega_c+6\omega_m)t}\cdots\end{bmatrix}\\&\times\begin{bmatrix}J_{-2}(\beta)e^{j(-2\omega_m)t}+J_2(\beta)e^{j(2\omega_m)t}+J_{-4}(\beta)e^{j(-4\omega_m)t}\\+J_4(\beta)e^{j(4\omega_m)t}+J_{-6}(\beta)e^{j(-6\omega_m)t}+J_6(\beta)e^{j(6\omega_m)t}\cdots\end{bmatrix}\\&=\frac{\gamma^2E_c}{4}\begin{bmatrix}-J_{-2}^2(\beta)e^{j(\omega_c-4\omega_m)t}-J_{-2}(\beta)J_2(\beta)e^{j\omega_ct}-J_{-2}(\beta)J_{-4}(\beta)e^{j(\omega_c-6\omega_m)t}\\-J_{-2}(\beta)J_4(\beta)e^{j(\omega_c+2\omega_m)t}-J_{-2}(\beta)J_{-6}(\beta)e^{j(\omega_c-8\omega_m)t}-J_{-2}(\beta)J_6(\beta)e^{j(\omega_c-4\omega_m)t}\\-J_2^2(\beta)e^{j(\omega_c+4\omega_m)t}-J_{-2}(\beta)J_2(\beta)e^{j\omega_ct}-J_2(\beta)J_{-4}(\beta)e^{j(\omega_c-2\omega_m)t}\\-J_2(\beta)J_4(\beta)e^{j(\omega_c+6\omega_m)t}-J_2(\beta)J_{-6}(\beta)e^{j(\omega_c-4\omega_m)t}-J_2(\beta)J_6(\beta)e^{j(\omega_c+8\omega_m)t}\\+J_{-4}^2(\beta)e^{j(\omega_c-8\omega_m)t}+J_{-4}(\beta)J_2(\beta)e^{j(\omega_c-2\omega_m)t}+J_{-2}(\beta)J_{-4}(\beta)e^{j(\omega_c-6\omega_m)t}\\+J_{-4}(\beta)J_4(\beta)e^{j\omega_ct}+J_{-4}(\beta)J_{-6}(\beta)e^{j(\omega_c-10\omega_m)t}+J_{-4}(\beta)J_6(\beta)e^{j(\omega_c+2\omega_m)t}\\+J_4^2(\beta)e^{j(\omega_c+8\omega_m)t}+J_4(\beta)J_2(\beta)e^{j(\omega_c+6\omega_m)t}+J_4(\beta)J_{-4}(\beta)e^{j(\omega_c-8\omega_m)t}\\+J_4(\beta)J_{-2}(\beta)e^{j(\omega_c+2\omega_m)t}+J_4(\beta)J_{-6}(\beta)e^{j(\omega_c-2\omega_m)t}+J_4(\beta)J_6(\beta)e^{j(\omega_c+10\omega_m)t}\\-J_{-6}^2(\beta)e^{j(\omega_c-12\omega_m)t}-J_{-6}(\beta)J_2(\beta)e^{j(\omega_c-4\omega_m)t}-J_{-6}(\beta)J_{-2}(\beta)e^{j(\omega_c-8\omega_m)t}\\-J_{-6}(\beta)J_4(\beta)e^{j(\omega_c-2\omega_m)t}-J_{-6}(\beta)J_{-4}(\beta)e^{j(\omega_c-10\omega_m)t}-J_{-6}(\beta)J_6(\beta)e^{j\omega_ct}\\-J_6^2(\beta)e^{j(\omega_c+12\omega_m)t}-J_6(\beta)J_{-2}(\beta)e^{j(\omega_c+4\omega_m)t}-J_6(\beta)J_2(\beta)e^{j(\omega_c+8\omega_m)t}\\-J_6(\beta)J_{-4}(\beta)e^{j(\omega_c+2\omega_m)t}-J_6(\beta)J_4(\beta)e^{j(\omega_c+10\omega_m)t}-J_6(\beta)J_{-6}(\beta)e^{j\omega_ct}\end{bmatrix}\\&=\frac{\gamma^2E_c}{4}\begin{bmatrix}\left(-2J_{-2}(\beta)J_2(\beta)+2J_{-4}(\beta)J_4(\beta)-2J_6(\beta)J_{-6}(\beta)\right)e^{j\omega_ct}\\+\left(-J_{-2}^2(\beta)-2J_2(\beta)J_{-6}(\beta)\right)e^{j(\omega_c-4\omega_m)t}+\left(-J_2^2(\beta)-2J_{-2}(\beta)J_6(\beta)\right)e^{j(\omega_c+4\omega_m)t}\end{bmatrix}.\end{aligned} \quad (2)$$

To achieve the W-band signal with frequency octupling, only the ±4th order sidebands must be retained, and all other sidebands must be eliminated. To curb the 0th-order optical sideband with output from MZM-b, the light splitter is set to (99:1), and the output light wave can be given as

$$E_{out} = \frac{\gamma^2 E_c}{4} \times \left[\left(-J_{-2}^2(\beta) - 2J_2(\beta)J_{-6}(\beta) \right) e^{j(\omega_c - 4\omega_m)t} + \left(-J_2^2(\beta) - 2J_{-2}(\beta)J_6(\beta) \right) e^{j(\omega_c + 4\omega_m)t} \right]. \quad (3)$$

After ±4th order sidebands beat frequency in a photodiode (PD), the detected electrical octupling mm-wave signal can be expressed as

$$I_{PD} = \zeta E_{out} \times E^*_{out} = \zeta E^2_c \left[\begin{matrix} \left(-J_{-2}^2(\beta) - 2J_2(\beta)J_{-6}(\beta) \right)^2 \\ + \left(-J_2^2(\beta) - 2J_{-2}(\beta)J_6(\beta) \right)^2 \end{matrix} \right] \cos^2 4\omega_m t$$
$$\propto \zeta E^2_c \left[\left(-J_{-2}^2(\beta) - 2J_2(\beta)J_{-6}(\beta) \right)^2 + \left(-J_2^2(\beta) - 2J_{-2}(\beta)J_6(\beta) \right)^2 \right] \cos 8\omega_m t. \quad (4)$$

Here ζ indicates the responsivity of the photodetector.

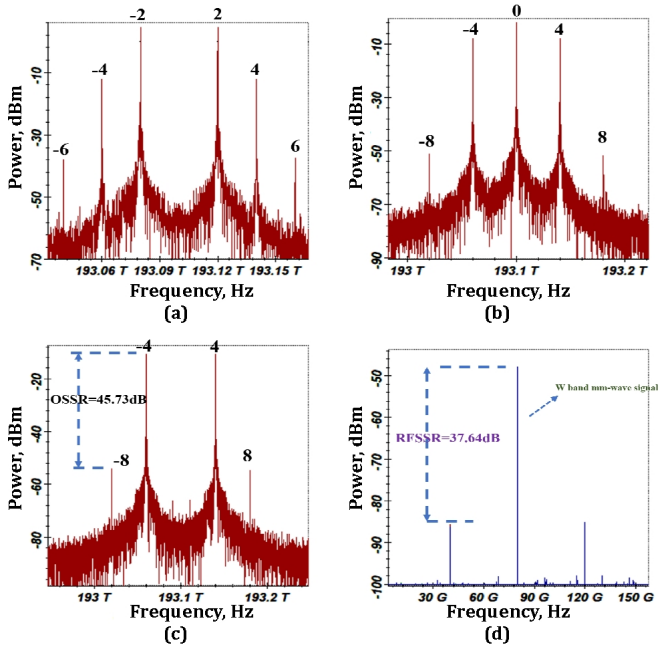

Fig. 2. Optical spectrum: (a) after MZM-a, (b) after MZM-b, (c) after eliminating the 0th-order harmonic; (d) RF spectrum of the generated W-band mm-wave signal with 80 GHz.

3. Simulation and result analysis

To demonstrate the accuracy and reliability of the presented W-band signal processing with an octupling generation scheme, a simulation was implemented based on computer OptiSystem software. In the system, a continuous optical carrier operates at a frequency of 193.1 THz, at the power of 20 dBm, and a linewidth of 10 MHz. The MZM-a and MZM-b, with a switching voltage of 3.2 V and an extinction ratio of 50 dB, are biased at the peak points. The RF driving signal has a frequency of 10 GHz. The amplitude of the RF driving signal is 2.4 V. The insertion loss for MZM is set to 5 dB. The responsivity of the photodetector is 1 A/W. The electrical phase shift of EPS is π/2.

Fig. 2a shows the optical spectra output by the MZM-a. One can find that the optical spectrums contain even order sidebands except 0th-order optical carrier, and the sidebands with order higher than six completely disappeared owing to low power, which consists of ±2nd order optical harmonics with ($\omega_c \pm 2\omega_m$) emerging at 193.08 THz and 193.12 THz, the ±4th order optical sidebands with ($\omega_c \pm 4\omega_m$) appearing at 193.06 THz and 193.14 THz, the ±6th order optical sidebands ($\omega_c \pm 6\omega_m$) appearing at 193.04 THz and 193.16 THz. Fig. 2b shows the optical spectrum at the outputs of the MZM-b. One can find the optical spectrums containing the ±4th order optical sidebands with ($\omega_c \pm 4\omega_m$) appearing at 193.06 THz and 193.14 THz and the ±8th order optical sidebands ($\omega_c \pm 8\omega_m$) appearing at 193.02 THz and 193.18 THz. After the second MZM, due to the influence of ± 2nd order, ± 4th order, and ± 6th order optical sidebands, the 0th order optical sidebands cannot be suppressed, as detailed in Eq. 2. By selecting a suitable beam splitter (99:1), the undesirable 0th harmonic can be eliminated, as shown in Fig. 2c. In Fig. 2c, a set of ± 4th-order light sidebands and a set of ± 8th-order light sidebands are seen. However, the ± 8th-order optical harmonics are irrelevant, as the optical sidebands are much lower than the ± 4th-order optical sidebands, and the OSSR reaches 45.73 dB, which would affect the quality of the generated millimeter wave signal.

The RF spectra of the generated W-band mm-wave signal with frequency octupling are shown in Fig. 2d. Then, the desired 80 GHz W-band signal is obtained. However, some spurious waves with frequencies at 40 and 120 GHz are derived due to the undesired 8th-order optical harmonics. Notwithstanding, the power of the generated W-band mm-wave signal at 80 GHz can reach 37.64 dB, which is far higher than derived spurious waves at 40 and 120 GHz.

Fig. 3 shows the influence of the extinction ratio for MZMs on OSSR and RFSSR. It can be seen from the figure that OSSR tends to flatten when the extinction ratio exceeds 47 dB, and RFSSR tends to flatten when the extinction ratio only needs to exceed 28 dB. In addition, by selecting MZM with a normal extinction ratio exceeding 20 dB in the experiment, the values of the system's OSSR and RFSSR can reach 14 and 20 dB, respectively, and therefore one can achieve good performance.

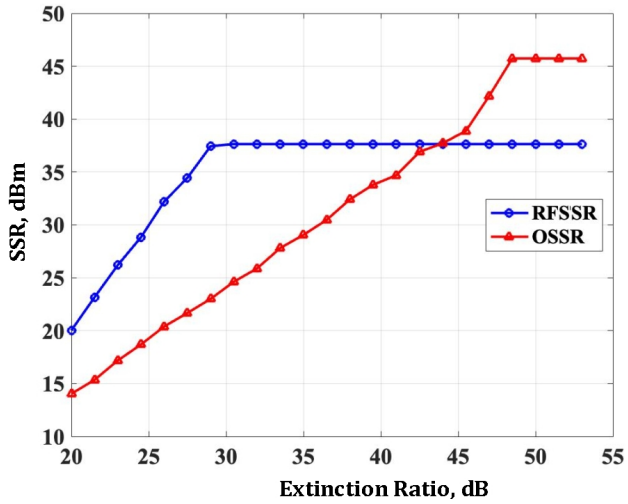

Fig. 3. The influence of the extinction ratio for MZMs on OSSR and RFSSR.

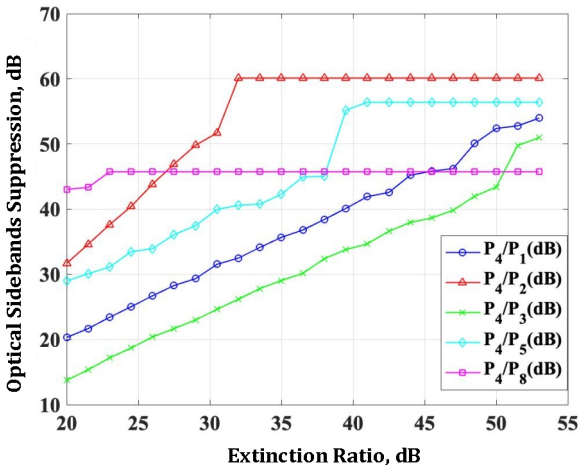

Fig. 4. The influence of extinction ratio on OSSR.

Due to the non-infinite extinction ratio of MZM, there may be residual odd-order harmonics. Fig. 4 indicates the influence of the extinction ratio on OSSR. The figure shows that as the extinction ratio increases, the optical sidebands suppression P_4/P_1, P_4/P_2, P_4/P_3, P_4/P_5, P_4/P_8 also increase synchronously. When the extinction ratio reaches 23 dB, P_4/P_8 first reaches stability, with a value of 45.73 dB. As the extinction ratio increases and reaches 31.5 dB, P_4/P_2 also reaches stability, with a value of 60 dB due to the suppression of the second-order optical sideband. When the extinction ratio reaches 39 dB, P4/P5 also reaches stability, with a value of 58 dB due to the suppression of the fifth-order optical sideband. As the extinction ratio increases and reaches 51 dB, P_4/P_1 and P_4/P_3 gradually exceed P_4/P_8, bringing the system's OSSR to 45.73. Therefore, if a modulator with an extinction ratio exceeding 50 dB is selected for this experiment, it will produce good results and achieve an OSSR of 45.73 dB. Therefore, in the experiment, it is necessary to choose MZM with a higher extinction ratio to improve the quality of the generated signal.

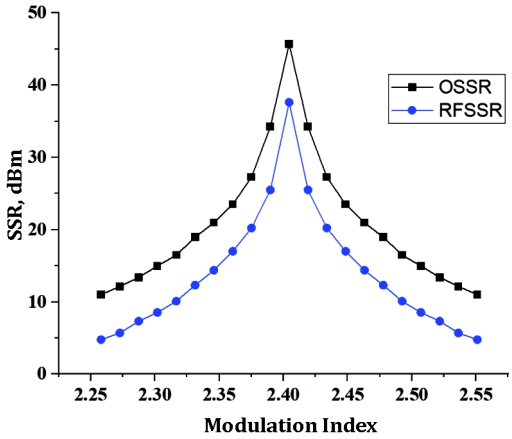

Fig.5. Effect of MI for MZMs on OSSR and RFSSR.

Fig. 5 shows the impact of MI for MZMs on OSSR and RFSSR. It can be seen from the figure that OSSR and RFSSR are sensitive to MI for MZMs. As the MI deviation from the standard value at 2.4 increases, the decrease in OSSR and RFSSR tends to flatten. When the

MI offset is controlled within 0.05, the system's OSSR and RFSSR values can reach 20 dB and 15 dB, respectively, and achieve good performance.

4. Conclusion

The paper proposes a modified approach to generating W-band mm-wave signals with octupling, in which an optical filter is unnecessary. The solution without optical filters can increase the tunable range of signal frequency. An integrated modulator consisting of two push-pull MZMs is employed. The octupling frequency signal generation depends on ±4th optical sidebands to beat frequency in the photodetector. For capturing ±4th optical sidebands, the two push-pull MZMs need to be biased at the peak point, and the MI of the MZMs is set to 2.4. OSSR can reach 45.73 dB, and RFSSR not less than 37.64 dB is achieved in the scheme. We analyzed the performance of the W-band mm-wave signal with 80 GHz in terms of OSSB and RFSSB when the extinction ratio and MI of the modulator are not ideal. With increased RF driving signal frequency, achieving a D-band or even a terahertz wave band is possible. Compared with previous schemes, this scheme has better and more stable performance.

Credit authorship contribution statement

Dongfei Wang: conceptualization, methodology, data curation, writing - original draft preparation, validation, visualization, investigation. **Yu Zhang**: funding acquisition; **Zufang Yang**: data curation; **Lan Zhang**: visualization; **Baohong Wu**: data curation, funding acquisition; **Xiaokun Yang**: editing, software; **Shuxia Yan**: funding acquisition; **Xiangqing Wang**: writing - reviewing and editing.

Declaration of competing interest

The authors declare that they have no known competing financial interests or personal relationships that could have appeared to influence the work reported in this paper.

Data availability

Data will be made available on request

Acknowledgments. This research was supported by the Jiangxi Provincial Natural Science Foundation (20232BAB212006) and the R&D Program of the Beijing Municipal Education Commission (KM202310015002), the Hubei Provincial Natural Science Foundation of China (2023AFB474) and the Open Project of Tianjin Key Laboratory of Optoelectronic Detection Technology and System (2023LOTDS019), the Open Project Program of Shanxi Key Laboratory of Advanced Semiconductor Optoelectronic Devices and Integrated Systems (2023SZKF21), the Henan Key Laboratory of Visible Light Communications (HKLVLC2023-B10), and the Special Fund of Advantageous and Characteristic Disciplines (Group) of Hubei Province. This research work was supported in part by the Scientific Research Project of Fuyang Normal University (2022KYQD0004) and Anhui Education Department, and the University Natural Science Research Project of Anhui Province (Grant 2022AH051338).

References

1. Dahiya, S. (2023). Performance analysis of millimeter wave-based radio over fiber system for next generation networks. *Journal of Optics*, 1-9.
2. Zheng, K., Yang, H., Ying, Z., Wang, P., & Hanzo, L. (2023). Vision-assisted millimeter-wave beam management for next-generation wireless systems: Concepts, solutions, and open challenges. *IEEE Vehicular Technology Magazine*, PP(*99*), 2-12.
3. Song, H., Huang, C., Li, H., Dai, L., Liu, Z., Yang, Y., Cheng, M., Yang, Q., Tang, M., Liu, D., & Deng, L. (2021). Asymmetric dual-SSB modulation for photonic co-frequency mm-wave signals generation and DSP-free receiver. *Optics Letters*, *46*(17), 4366-4369.

4. Li, J. L., Zhao, F., & Yu, J. (2020). D-band millimeter wave generation and transmission though radio-over-fiber system. *IEEE Photonics Journal*, *12*(2), 1-8.
5. Wang, D., Wang, X., Yang, X., Gao, F., Zhang, L., Yang, Z., & Wu, B. (2023). Photonic filter-free adjustable frequency sextupling scheme for V-band vector mm-wave signal generation based on a DP-MZM with precoding. *Optics Communications*, 129633.
6. Liu, C., Zhou, W., & Yu, J. (2022). Photonics aided vector millimeter-wave signal generation without DAC at W-band. *Optical Fiber Technology*, *70*, 102883.
7. Zhao, L., Zhang, R., Zhou, W., Shen, S., Xiao, J., Chang, G. K., & Yu, J. (2021). Probabilistic shaping with pre-equalization in W-band MM-wave communication system with heterodyne coherent detection. *Optical Fiber Technology*, *61*, 102345.
8. Althuwayb, A. A., Alibakhshikenari, M., Virdee, B. S., Benetatos, H., Rashid, N., Kaaniche, K., Atitallah, A. B. & Elhamrawy, O. I. (2023). Design technique to mitigate unwanted coupling in densely packed radiating elements of an antenna array for electronic devices and wireless communication systems operating in the millimeter-wave band. *AEU-International Journal of Electronics and Communications*, *159*, 154464.
9. Oyerinde, O. O., Flizikowski, A., & Marciniak, T. (2022). Compressive sensing-based channel estimation schemes for wideband millimeter wave wireless communication systems. *Computers and Electrical Engineering*, *104*, 108452.
10. Arsalan, M., Santra, A., & Issakov, V. (2022). RadarSNN: A resource efficient gesture sensing system based on mm-wave radar. *IEEE Transactions on Microwave Theory and Techniques*, *70*(4), 2451-2461.
11. Ma, Z., Choi, J., & Sohn, H. (2023). Continuous bridge displacement estimation using millimeter-wave radar, strain gauge and accelerometer. *Mechanical Systems and Signal Processing*, *197*, 110408.
12. Gillani, N., Arslan, T., & Mead, G. (2023). An Unobtrusive Method for Remote Quantification of Parkinson's and Essential Tremor using mm-Wave Sensing. *IEEE Sensors Journal*, 23(9), 10118-10131.
13. Ni, Z., & Huang, B. (2022). Gait-based person identification and intruder detection using mm-wave sensing in multi-person scenario. *IEEE Sensors Journal*, *22*(10), 9713-9723.
14. Murphy, K. S. J., Appleby, R., Sinclair, G., McClumpha, A., Tatlock, K., Doney, R., & Hutcheson, I. (2002, October). Millimetre wave aviation security scanner. In *Proceedings. 36th Annual 2002 International Carnahan Conference on Security Technology* (pp. 162-166). IEEE.
15. Tajdini, M. M., & Rappaport, C. M. (2021). Nominal body contour reconstruction for millimeter-wave characterization of suicide bomber explosives. *IEEE Transactions on Antennas and Propagation*, *70*(4), 2960-2968.
16. Li, B., Zhang, L., Zhang, Q., Xin, X., Pan, X., Zhang, W., Tian, Q., Tao, Y., Liu, N., Wang, Y. & Tian, F. (2019). Flexible photonic generation of frequency multiplication millimeter-wave vector signal based on dynamic pre-coding algorithm with dispersion compensation. *Optics Communications*, *435*, 232-238.
17. Chen, H., Ning, T., Li, J., Pei, L., Yuan, J., Zheng, J., & Liu, L. (2018). Optical millimeter-wave generation with tunable multiplication factors and reduced power fluctuation by using cascaded modulators. *Optics & Laser Technology*, *103*, 206-211.
18. Baskaran, M., Prabakaran, R., & Gayathri, T. S. (2019). Photonic generation of frequency 16-tupling Millimeter wave signal using polarization property without an optical filter. *Optik*, *184*, 348-355.
19. Wang, D., Tang, X., Xi, L., Zhang, X., & Fan, Y. (2019). A filterless scheme of generating frequency 16-tupling millimeter-wave based on only two MZMs. *Optics & Laser Technology*, *116*, 7-12.
20. Chen, X., Xia, L., & Huang, D. (2017). A filterless 24-tupling optical millimeter-wave generation and RoF distribution. *Optik*, *147*, 22-26.
21. Ramos, R. T., & Seeds, A. J. (1992). Fast heterodyne optical phase-lock loop using double quantum well laser diodes. *Electronics Letters*, *1*(28), 82-83.
22. Cliché, J. F., Shillue, B., Tetu, M., & Poulin, M. (2007, June). A 100-GHz-tunable photonic millimeter wave synthesizer for the Atacama Large Millimeter Array radiotelescope. In *2007 IEEE/MTT-S International Microwave Symposium* (pp. 349-352). IEEE.
23. Baskaran, M., & Madhan, M. G. (2014). A novel approach for simultaneous millimeter wave generation and high bit rate data transmission for Radio over Fiber (RoF) systems. *Optik*, *125*(21), 6347-6351.
24. Zheng, H., Liu, S., Li, X., Wang, W., & Tian, Z. (2009). Generation and transmission simulation of 60 G millimeter-wave by using semiconductor optical amplifiers for radio-over-fiber systems. *Optics communications*, *282*(22), 4440-4444.
25. Han, S. H., & Park, C. S. (2011, July). Photonic millimeter-wave carrier generation using stimulated Brillouin scattering and four wave mixing for MMW-over-fiber system. In *16th Opto-Electronics and Communications Conference* (pp. 539-540). IEEE.
26. Wang, D., Xi, L., Tang, X., Zhang, X., & Gao, N. (2020). A simple photonic precoding-less scheme for vector millimeter-wave signal generation based on a single phase modulator. *Results in Physics*, *19*, 103412.
27. Li, X., Xu, Y., Xiao, J., & Yu, J. (2016). W-band millimeter-wave vector signal generation based on precoding-assisted random photonic frequency tripling scheme enabled by phase modulator. *IEEE Photonics Journal*, *8*(2), 1-10.
28. Zhou, W., & Qin, C. (2017). Simultaneous generation of 40, 80 and 120 GHz optical millimeter-wave from one Mach-Zehnder modulator and demonstration of millimeter-wave transmission and down-conversion. *Optics Communications*, *398*, 101-106.
29. Wang, Y., Liu, C., & Yu, J. (2020). Dispersion-tolerant millimeter-wave signal generation by a single modulator. *Optics Communications*, *475*, 126204.

30. Zhu, Z., Zhao, S., Yao, Z., Tan, Q., Li, Y., Chu, X., Shi, L. & Zhang, X. (2012). Optical millimeter-wave signal generation by frequency quadrupling using one dual-drive Mach–Zehnder modulator to overcome chromatic dispersion. *Optics Communications*, *285*(13-14), 3021-3026.
31. Li, X., Yu, J., Zhang, Z., Xiao, J., & Chang, G. K. (2015). Photonic vector signal generation at W-band employing an optical frequency octupling scheme enabled by a single MZM. *Optics Communications*, *349*, 6-10..
32. Zhu, Z., Zhao, S., Zheng, W., Wang, W., & Lin, B. (2015). Filterless frequency 12-tupling optical millimeter-wave generation using two cascaded dual-parallel Mach–Zehnder modulators. *Applied Optics*, *54*(32), 9432-9440.
33. Shang, Y., Feng, Z., Cao, C., Huang, Z., Wu, Z., Xu, X., & Geng, J. (2022). A using remodulation filterless scheme of generating frequency 32-tupling millimeter-wave based on two DPMZMs. *Optics & Laser Technology*, *148*, 107793.
34. Zhang, W., Wen, A., Gao, Y., Shang, S., Zheng, H., & He, H. (2017). Filterless frequency-octupling mm-wave generation by cascading Sagnac loop and DPMZM. *Optics & Laser Technology*, *97*, 229-233.
35. Chen, X., Li, Z., Ba, W., Dai, S., Liang, J., & Xiao, H. (2023). A novel method to generate and transmit 40-tupling frequency millimeter wave over fiber based on remodulation of MZMs. *Heliyon*, *9*(3), e14221.
36. Wang, C., Song, K., Li, M., Yi, Y., Zhou, M., & Wu, J. Generation of frequency 16-tupling millimeter wave without filtering based on cascaded Mach–Zehnder modulator. *Microwave and Optical Technology Letters*.
37. Shanmugapriya, G. (2017). Frequency16-tupled optical millimeter wave generation using dual cascaded MZMs and 2.5 Gbps RoF transmission. *Optik*, *140*, 338-346.
38. Chen, X., Li, Z., Liu, X., Ba, W., & Dai, S. (2022). Research on 32-tupling frequency terahertz wave generation based on Mach-Zehnder modulators cascaded. *Optik*, *270*, 170027.
39. Li, Y., Zhu, R., Xu, E., & Zhang, Z. (2023). Frequency-Doubling Brillouin Optoelectronic Oscillator with Variable Optical Attenuator. *IEEE Photonics Technology Letters*.
40. Ma, J., Wen, A., & Tu, Z. (2019). Filter-free photonic microwave upconverter with frequency quadrupling. *Applied Optics*, *58*(28), 7915-7920.
41. Zhang, W., Wen, A., Gao, Y., Shang, S., Zheng, H., & He, H. (2017). Filterless frequency-octupling mm-wave generation by cascading Sagnac loop and DPMZM. *Optics & Laser Technology*, *97*, 229-233.
42. Chen, Y., Wen, A., & Shang, L. (2010). Analysis of an optical mm-wave generation scheme with frequency octupling using two cascaded Mach–Zehnder modulators. *Optics Communications*, *283*(24), 4933-4941.

Dongfei Wang, Yu Zhang, Zufang Yang, Lan Zhang, Baohong Wu, Xiaokun Yang Shuxia Yan, Xiangqing Wang. (2024). A New Filterless W-Band Millimeter Wave Signals Generation Scheme with Frequency Octupling Based on Cascaded Mach–Zehnder Modulators. *Ukrainian Journal of Physical Optics*, *25*(1), 01085 – 01093.
doi: 10.3116/16091833/Ukr.J.Phys.Opt.2024.01085

Анотація. *Існуючі діапазони частот, такі як С-діапазон і L-діапазон, стають все більш переповненими і не можуть задовольнити зростаючий попит на високошвидкісні послуги передачі даних. Щоб подолати перевантаження спектру та задовольнити майбутні потреби, а також подолати вузькі місця традиційних електронних методів, ми модифікували підхід для генерації сигналів мм-хвиль W-діапазону з восьмикратним збільшенням частоти без використання оптичного фільтра. Для генерації сигналу W-діапазону використовується один вбудований модулятор, що складається з двох послідовно з'єднаних двотактних модуляторів Маха-Цендера (ММЦ). Генерація сигналу з восьмикратним помноженням частоти залежить від ±4 оптичних бічних смуг і смуги частот биття фотодетектора. Для захоплення ±4-ї оптичної бічної смуги точка зміщення двох двотактних ММЦ повинна відповідати піковій точці, а індекс модуляції двох ММЦ має бути одночасно встановлений на 2,4. Ми провели детальний математичний аналіз та комп'ютерне моделювання запропонованої схеми і продемонстрували її коректність. Показано, що коефіцієнт оптичного пригнічення бокової смуги становить не менше 45,73 дБ, а коефіцієнт пригнічення бокової радіочастотної смуги може досягати 37,64 дБ.*

Ключові слова: *W-діапазон, генерація сигналу міліметрового діапазону, восьмикратне збільшення частоти, модулятор Маха–Цендера.*